Dual effects of Ral-activated pathways on p27 localization and TGF-β signaling

Keren Tazat[a], Meirav Harsat[a], Ayelet Goldshmid-Shagal[a], Marcelo Ehrlich[b], and Yoav I. Henis[a]
[a]Department of Neurobiology and [b]Department of Cell Research and Immunology, George S. Wise Faculty of Life Sciences, Tel Aviv University, Tel Aviv 69978, Israel

ABSTRACT **Constitutive activation or overactivation of Ras signaling pathways contributes to epithelial tumorigenesis in several ways, one of which is cytoplasmic mislocalization of the cyclin-dependent kinase inhibitor p27^{Kip1} (p27). We previously showed that such an effect can be mediated by activation of the Ral-GEF pathway by oncogenic N-Ras. However, the mechanism(s) leading to p27 cytoplasmic accumulation downstream of activated Ral remained unknown. Here, we report a dual regulation of p27 cellular localization by Ral downstream pathways, based on opposing effects via the Ral effectors RalBP1 and phospholipase D1 (PLD1). Because RalA and RalB are equally effective in mislocalizing both murine and human p27, we focus on RalA and murine p27, which lacks the Thr-157 phosphorylation site of human p27. In experiments based on specific RalA and p27 mutants, complemented with short hairpin RNA–mediated knockdown of Ral downstream signaling components, we show that activation of RalBP1 induces cytoplasmic accumulation of p27 and that this event requires p27 Ser-10 phosphorylation by protein kinase B/Akt. Of note, activation of PLD1 counteracts this effect in a Ser-10–independent manner. The physiological relevance of the modulation of p27 localization by Ral is demonstrated by the ability of Ral-mediated activation of the RalBP1 pathway to abrogate transforming growth factor-β–mediated growth arrest in epithelial cells.**

Monitoring Editor
Carl-Henrik Heldin
Ludwig Institute for Cancer Research

Received: Jan 3, 2013
Revised: Mar 22, 2013
Accepted: Apr 1, 2013

INTRODUCTION

The cyclin-dependent kinase (CDK) inhibitor p27^{Kip1} (p27) belongs to the Cip/Kip family of CDK inhibitors, which inhibit cyclin D–, E–, A–, and B–dependent kinases (Sherr and Roberts, 1999). p27 has a major role in cell cycle arrest, regulating progression through the G1/S phases (Sherr and Roberts, 1999). Loss of cell cycle inhibition by p27 has been reported in many cancers and correlates with tumor aggressiveness and poor prognosis (Loda *et al.*, 1997; Tsukamoto *et al.*, 2001; Wander *et al.*, 2011). This loss is mediated mainly by p27 degradation or translocation to the cytoplasm, where it is sequestered away from the nuclear cyclin–CDK complexes (Pagano *et al.*, 1995; Bloom and Pagano, 2003; Vlach *et al.*, 1997; Liu *et al.*, 2000; Rodier *et al.*, 2001; Liang *et al.*, 2002; Viglietto *et al.*, 2002; Kfir *et al.*, 2005; Besson *et al.*, 2008; Chu *et al.*, 2008). Translocation of p27 to the cytoplasm is mediated by its phosphorylation on Ser-10 (Rodier *et al.*, 2001; Boehm *et al.*, 2002; Ishida *et al.*, 2002; Besson *et al.*, 2006). Human p27 cytoplasmic translocation can also be mediated by phosphorylation at Thr-157 (Liang *et al.*, 2002; Shin *et al.*, 2002; Viglietto *et al.*, 2002), which is missing in murine p27.

Constitutive activation or overactivation of Ras signaling pathways is encountered in many tumors (Bos, 1989). Induction of p27 cytoplasmic mislocalization was reported as a mechanism by which Ras overactivation can interfere with normal cell cycle arrest. Although such an effect can be mediated by phosphorylation of human (but not murine) p27 on Thr-157 by protein kinase B/Akt (Liang *et al.*, 2002; Shin *et al.*, 2002; Viglietto *et al.*, 2002), an alternative mechanism is activation of Ral via the Ral-GEF pathway to induce cytoplasmic mislocalization of both human and murine p27 (Kfir *et al.*, 2005). However, Ral proteins can activate several downstream pathways, whose role in regulating p27 subcellular localization remained unclear; unraveling these roles is a major aim of the present study.

This article was published online ahead of print in MBoC in Press (http://www.molbiolcell.org/cgi/doi/10.1091/mbc.E13-01-0007) on April 10, 2013.

Address correspondence to: Yoav I. Henis (henis@post.tau.ac.il).

Abbreviations used: BrdU, bromodeoxyuridine; CDK, cyclin-dependent kinase; DN, dominant negative; GαM, goat anti-mouse; GαR, goat anti-rabbit; HA, influenza hemagglutinin; p27, cyclin-dependent kinase inhibitor p27^{Kip1}; PLD, phospholipase D; TGF-β, transforming growth factor-β; WT, wild type.

The RalA and RalB proteins, which share 85% protein sequence identity (Feig, 2003; van Dam and Robinson, 2006), belong to the Ras-like small G protein family. Both have been implicated in Ras-mediated oncogenesis, with RalA mediating anchorage-independent growth and RalB promoting cell survival, migration, and metastasis (Chien and White, 2003; Bodemann and White, 2008; Lim *et al.*, 2005, 2006; Oxford *et al.*, 2005; Rosse *et al.*, 2006; Martin *et al.*, 2011). Ral proteins signal via binding to several distinct effector proteins; the major and best-characterized Ral effectors are RalBP1 (RLIP76), which is a Ral-activated Rho-GAP acting mainly on Cdc42 and Rac, the Sec5 and Exo84 subunits of the exocyst complex, and phospholipase D1 (PLD1; Cantor *et al.*, 1995; Luo *et al.*, 1997; Moskalenko *et al.*, 2002; Feig, 2003; van Dam and Robinson, 2006). These pathways regulate endocytosis, exocytosis, actin organization, and gene expression (Feig, 2003; van Dam and Robinson, 2006). Both RalBP1 and the exocyst subunits are involved in oncogenic Ras signaling (Lim *et al.*, 2005; Issaq *et al.*, 2010). In contrast, PLD1 exhibits cell context–dependent protumorigenic and antitumorigenic effects; whereas it was reported to be involved in Ras-mediated cell transformation (Jiang *et al.*, 1995; Min *et al.*, 2001), other studies suggested that it has prodifferentiation roles (Nakashima and Nozawa, 1999; Klein, 2005; Yoon and Chen, 2008).

In a previous study, we showed that cytoplasmic mislocalization of p27 after activation of the Ral-GEF pathway by oncogenic N-Ras perturbs growth inhibition by transforming growth factor-β (TGF-β) in epithelial cells (Kfir *et al.*, 2005). After TGF-β stimulation, Smad2/3 proteins are phosphorylated by the type I TGF-β receptor, translocated to the nucleus with Smad4, and regulate gene transcription (Wrana *et al.*, 1992; Shi and Massague, 2003; Schmierer and Hill, 2007). To inhibit proliferation, TGF-β suppresses the expression of c-Myc, cyclin A, Cdc25A, and CDK4/6 (Pietenpol *et al.*, 1990; Ewen *et al.*, 1993; Iavarone and Massague, 1997; Tsubari *et al.*, 1999; Derynck *et al.*, 2001) and induces the CDK inhibitors $p15^{Ink4B}$ (prominent in Mv1Lu mink lung epithelial cells) and $p21^{Waf/Cip1}$ (Hannon and Beach, 1994; Datto *et al.*, 1995; Hu *et al.*, 1998). $p15^{Ink4B}$ releases p27 from CDK4/6, inhibiting CDK2 (Reynisdottir and Massague, 1997; Sherr and Roberts, 1999), whose activity in complex with cyclin E and the resulting hyperphosphorylation of the retinoblastoma protein are required for G1/S transition (Harbour *et al.*, 1999; Sherr and Roberts, 1999). Therefore p27 sequestration in the cytoplasm disrupts TGF-β–mediated growth arrest, providing a physiologically relevant readout for the effect of Ral-mediated p27 mislocalization.

In the present work, we investigate the distinct roles of the major Ral downstream signaling pathways (RalBP1, the exocyst, and PLD1) in regulating p27 subcellular localization and their effects on TGF-β growth arrest. Because RalA and RalB were equally effective in translocating p27 to the cytoplasm, we chose RalA for further investigation. Our results reveal a delicate balance between the RalBP1 pathway, which mediates p27 translocation to the cytoplasm and requires p27 phosphorylation at Ser-10 by Akt, and the PLD1 pathway, which is independent of Ser-10 phosphorylation and supports nuclear localization of p27. The physiological relevance of Ral-mediated p27 mislocalization via the RalBP1 pathway is demonstrated by its ability to abrogate TGF-β–mediated growth arrest in epithelial cells.

RESULTS

Both RalA and RalB induce accumulation of murine and human p27 in the cytoplasm

We previously demonstrated (Liu *et al.*, 2000; Kfir *et al.*, 2005) that expression of constitutively active N-Ras(Q61K) in mink lung epithelial cells (Mv1Lu) induces mislocalization of p27 to the cytoplasm, sequestering p27 in the cytoplasm separate from CDK2 and disrupting TGF-β–mediated growth arrest. We further demonstrated that these effects are mediated via activation of Ral-GEF (Kfir *et al.*, 2005). However, the Ral proteins, which are the immediate targets of Ral-GEF, activate numerous downstream signaling pathways, and the mechanisms by which distinct Ral downstream pathways regulate the intracellular distribution of p27 remained unknown; this issue was at the center of the present study.

First, we studied the effects of wild-type (WT) RalA and RalB and their constitutively active forms—RalA(Q72L) and RalB(Q72L)—on p27 localization. In accord with our previous results (Kfir *et al.*, 2005), transient expression of RalA or RalB in Mv1Lu mink lung epithelial cells induced cytoplasmic mislocalization of transfected human and murine p27 (Figure 1, A–C), as well as of endogenous p27 (Figure 1D). Of note, a stronger effect was mediated by the constitutively active Ral isoforms. These observations are not unique to Mv1Lu cells, as shown by the similar effects in transfected Cos7 cells (Figure 1E). Because RalA and RalB were equally effective in shifting p27 to the cytoplasm, we focused in further experiments on RalA and RalA-derived mutants. In these studies, we used murine p27 because it lacks Thr-157 found in human p27, whose phosphorylation by Akt may also induce cytoplasmic mislocalization of human (but not murine) p27 (Liang *et al.*, 2002; Shin *et al.*, 2002; Viglietto *et al.*, 2002).

Cytoplasmic mislocalization of p27 by Ral is induced via RalBP1

To identify which RalA effector pathways are involved in p27 mislocalization, we cotransfected Mv1Lu cells with murine GFP-p27 together with empty vector (control), constitutively active N-Ras(Q61K), or vectors encoding various human RalA constructs. The RalA mutants used were RalA(Q72L), dominant-negative (DN)–RalA, and double mutants of RalA(Q72L) containing a second mutation that renders them unable to activate one of the three major Ral pathways: 1) RalA(Q72L/ΔN11), defective in PLD1 binding (Jiang *et al.*, 1995); 2) RalA(Q72L/D49N), defective in RalBP1 binding (Cantor *et al.*, 1995); and 3) RalA(Q72L/D49E), defective in binding Sec5 and Exo84 of the exocyst complex (Moskalenko *et al.*, 2002, 2003). In accord with our previous results, N-Ras(Q61K) and RalA(Q72L) were highly effective in mislocalizing GFP-p27 to the cytoplasm (Figure 2, A and B). RalA(Q72L/ΔN11) was nearly as effective, indicating that binding of RalA to PLD1 and downstream signaling from PLD1 are not required for RalA-mediated cytoplasmic accumulation of p27. In contrast, the RalBP1-defective RalA(Q72L/D49N) mutant (and DN-RalA) completely failed to mislocalize GFP-p27 (Figure 2, A and B). The mutant defective in exocyst activation, RalA(Q72L/D49E), was also impaired in mediating p27 mislocalization to the cytoplasm but to a lesser degree than the RalBP1-defective mutant. These effects were not limited to transiently expressed GFP-p27 or to Mv1Lu cells, since similar results were obtained with the entire spectrum of mutants for endogenous p27 in Mv1Lu cells (Figure 2C) and for murine GFP-p27 in Cos7 cells (Figure 2D). These findings suggest that the RalBP1 and the exocyst pathways, but not the PLD1 pathway, might be required for cytoplasmic sequestration of p27.

Because the RalA mutations that inactivate its interactions with RalBP1 and the exocyst complex involve the same amino acid (D49), it is possible that they are not fully specific, and a further discrimination between the RalBP1 and the exocyst pathways is desired. To that extent, we used short hairpin RNA (shRNA) to reduce the expression of either RalBP1 or Sec5. The RalBP1 shRNA was highly effective in reducing RalBP1 expression in Mv1Lu cells relative to scrambled shRNA (Figure 3A), leading to a nearly complete loss of the ability of RalA(Q72L) to induce mislocalization of GFP-p27 (Figure 3, C and E). On the other hand, reduction of the Sec5 mRNA

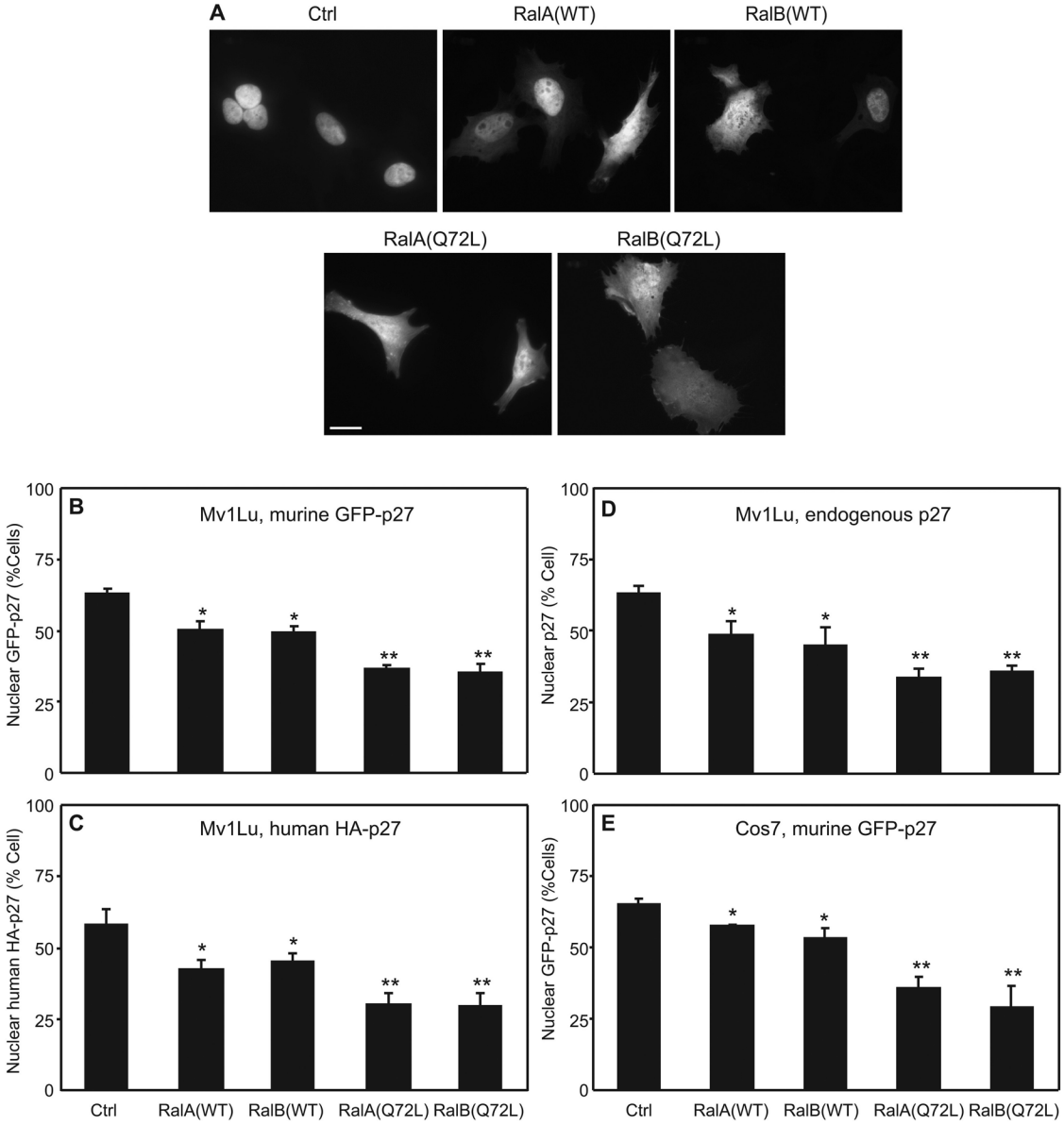

FIGURE 1: Effects of WT and constitutively active RalA and RalB on p27 localization. Mv1Lu cells (A–D) or Cos7 cells (E) were cotransfected with murine GFP-p27 (A, B, and E), human HA-p27 (C), or pEGFP (as transfection marker; D) together with a sixfold excess of the indicated Ral expression vectors or empty vector (Ctrl). After 24 h, they were fixed and either directly mounted for fluorescence imaging (GFP; A, B, E) or permeabilized (0.2% Triton X-100) and immunostained against HA-p27 (C) or endogenous p27 (D). To label HA-p27, the cells were incubated successively with 1) rabbit anti-HA (4 μg/ml); 2) biotin-GαR IgG (5 μg/ml); and 3) Cy3-streptavidin (1.2 μg/ml). Endogenous p27 was labeled by successive incubation with 1) rabbit anti-p27 (1.25 μg/ml); 2) biotin-GαR IgG (5 μg/ml); and 3) Cy3-streptavidin (1.2 μg/ml). (A) Typical images of murine GFP-p27 in Mv1Lu cells. Bar, 20 μm. Bar graphs (B–E) show the quantification of the percentage of cells with predominantly nuclear localization of (B) murine GFP-p27 in Mv1Lu cells, (C) human HA-p27 in Mv1Lu cells, (D) endogenous Mv1Lu p27, and (E) murine GFP-p27 in Cos7 cells. Bars, means ± SEM of three samples in each case, scoring 100 transfected cells per sample for nuclear and cytoplasmic localization of p27. Asterisks denote significant differences from the control (**$p < 0.02$; *$p < 0.04$; Student's t test). Mainly nuclear localization is evident for the control; WT RalA and RalB reduced the level of nuclear p27, a phenomenon that became stronger with the Q72L mutants. To verify equivalent expression levels of the untagged transfected constructs, we measured their relative mRNA levels by real time RT-PCR, using a primer localized to the coding sequence of RalA or RalB and a primer preceding the poly(A) sequence in the expression plasmid (see *Materials and Methods*). The mRNA levels of RalA(Q72L) and RalB(Q72L) were comparable to those of their WT counterparts.

level by Sec5 shRNA (Figure 3B) had no effect on p27 mislocalization by RalA(Q72L) (Figure 3, D and F). We conclude that the RalBP1 pathway is essential for Ral-mediated sequestration of p27 in the cytoplasm.

Next we explored whether activation of RalBP1 is sufficient to translocate p27 to the cytoplasm. Because RalBP1 is activated by its recruitment to the membrane, fusion of RalBP1 to the N-terminal membrane anchor of RalA (last 30 residues) results in a constitutively

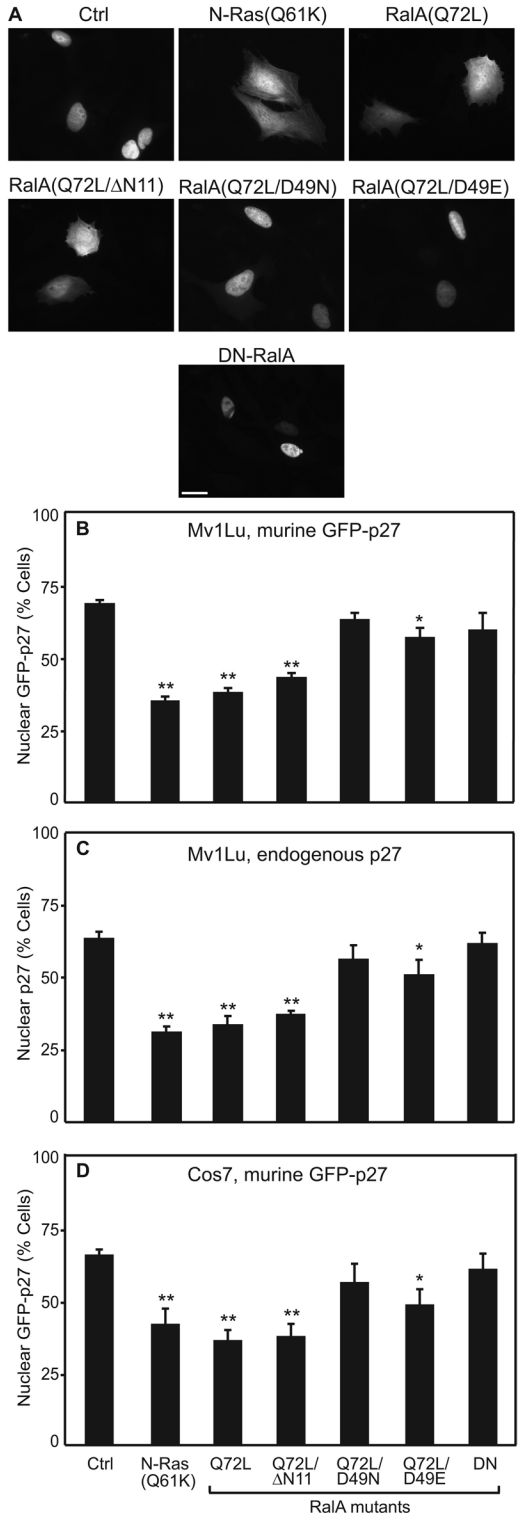

FIGURE 2: Effects of constitutively active RalA effector mutants on p27 localization. Mv1Lu cells (A–C) or Cos7 cells (D) were cotransfected with murine GFP-p27 (A, B, D) or pEGFP (transfection marker; C) together with an excess (sixfold) of the indicated vectors (Ctrl, empty vector). After 24 h, the cells were fixed and either directly mounted for imaging GFP-p27 (A, B, D) or permeabilized and stained for endogenous p27 as in Figure 1 (C). (A) Typical images of murine GFP-p27 cellular localization in Mv1Lu cells. Bar, 20 μm. Bar graphs (B–D) depict the quantification of the percentage of cells showing mainly nuclear distribution of (B) murine GFP-p27 in Mv1Lu cells, (C) endogenous Mv1Lu p27, and (D) murine GFP-p27 in Cos7 cells. Bars, means ± SEM of about six samples in each case, scoring 100 transfected cells per sample. Asterisks denote significant differences from the control (**$p < 0.02$; *$p < 0.04$; Student's *t* test). p27 was mainly nuclear in the control. Constitutively active RalA(Q72L) and RalA(Q72L/ΔN11) shifted p27 to the cytoplasm as effectively as N-Ras(Q61K). In contrast, RalA(Q72L/D49N) failed to translocate p27 to the cytoplasm, similar to DN-RalA. RalA(Q72L/D49E) was also defective in inducing p27 cytoplasmic localization, albeit to a somewhat lesser extent than RalA(Q72L/D49N) (the RalBP1-defective mutant). To confirm that the expression levels of the various RalA constructs are similar, their relative mRNA levels were measured by real-time RT-PCR as described in Figure 1, using the primers described under *Materials and Methods*; the mRNA levels of all RalA mutants were similar within a factor of 1.5 ($p > 0.1$, Student's *t* test).

active RalBP1-RalA fusion protein (Kashatus *et al.*, 2011). Transient expression of RalBP1-RalA in Mv1Lu cells induced cytoplasmic localization of p27 as effectively as RalA(Q72L) (Figure 4). Of interest, whereas overexpression of RalBP1(WT) induced lower but detectable cytoplasmic mislocalization of p27 (most likely due to some level of activation of the WT protein in the presence of serum), an RalBP1 mutant lacking GAP activity—RalBP1(R208L/K244R)—was not only ineffective, but even increased the percentage of cells with nuclear GFP-p27, suggesting that it might possess some dominant-negative characteristics (Figure 4). These results demonstrate that active RalBP1 is sufficient to induce p27 mislocalization without a need for coactivation of the exocyst pathway.

Inhibition of PLD1 leads to translocation of p27 to the cytoplasm

The results with the RalA(Q72L/ΔN11) mutant (defective in binding PLD1) indicate that the Ral-PLD1 pathway is dispensable for p27 cytoplasmic mislocalization by RalA. To further explore the potential roles of the PLD1 pathway in modulating p27 localization, we investigated the effects of DN-PLD1 and DN-PLD2 on green fluorescent protein (GFP)–p27 cellular localization. DN-PLD1, but not DN-PLD2, induced p27 cytoplasmic localization (Figure 5, A and B) to the same extent as RalA(Q72L/ΔN11) (see Figure 2), in line with the report that the PLD isoform that interacts with Ral is PLD1 (Hammond *et al.*, 1995).

An additional demonstration that inhibition of PLD activity shifts p27 to the cytoplasm was provided by studies based on inhibiting PLD by 1-butanol. In the presence of this primary alcohol, PLD generates a phosphatidylalcohol product instead of phosphatidic acid (Bi *et al.*, 1997; Frohman *et al.*, 1999; Boucrot *et al.*, 2006). As shown in Figure 5C, PLD inhibition by 1-butanol (but not by iso-butanol, which does not affect PLD) in control cells induced p27 cytoplasmic mislocalization. Moreover, 1-butanol inhibition of PLD induced a minor but significant increase in GFP-p27 cytoplasmic mislocalization by either N-Ras(Q61K) or RalA(Q72L), in line with a contribution of PLD to the nuclear localization of p27.

To validate the foregoing findings, we stably transfected human lung epithelial A549 cells with PLD1 shRNA (targeted to human PLD1) in pEGFP vector, followed by preparative sorting of GFP-positive cells. The sorted cells displayed very low PLD1 levels as compared with cells sorted after transfection by a vector encoding an unrelated shRNA sequence (Figure 6A). Of note, the reduced PLD1 expression was accompanied by sequestration of p27 in the cytoplasm (Figure 6, B and C). Taken together, the findings in Figures 5 and 6 suggest that PLD1 is required for the normal, mainly nuclear, localization of p27, and disruption of PLD1 activity can tilt the balance in favor of p27 cytoplasmic localization.

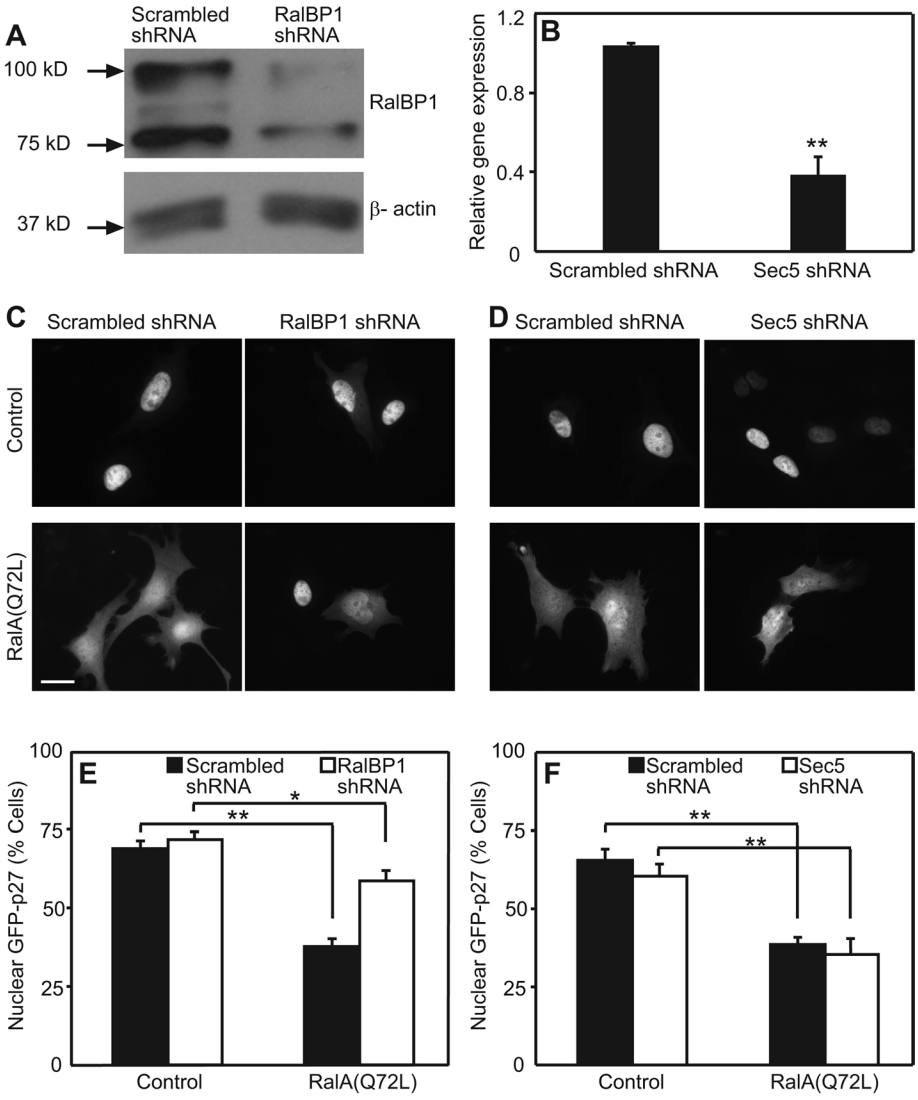

FIGURE 3: Knockdown of RalBP1 but not Sec5 disrupts RalA(Q72L)-mediated p27 cytoplasmic mislocalization. Mv1Lu cells were infected with retroviruses encoding RalBP1 shRNA, Sec5 shRNA, or scrambled sequences. (A) Western blotting shows effective knockdown of endogenous RalBP1. Quantification after normalization to the loading control (β-actin) yielded reduction ± SEM by 80 ± 4% ($n = 3$). (B) Real-time RT-PCR analysis of the relative Sec5 mRNA level shows a 65% reduction (means ± SEM, $n = 5$; $^{**}p < 0.001$). (C, D) Typical images of murine GFP-p27 localization. The cells were transfected with vectors encoding murine GFP-p27 together with an excess (sixfold) of RalA(Q72L) or empty vector (control), fixed, and imaged 24 h posttransfection. Bar, 20 μm. (E, F) Quantification of GFP-p27 localization. Bars, means ± SEM ($n = 4$ or 5), scoring 100 transfected cells per sample. Asterisks indicate significant differences ($^{**}p < 0.001$; $^{*}p < 0.02$; Student's t test) from the relevant control. RalA(Q72L) was highly effective in mislocalizing murine GFP-p27 in cells infected with viruses encoding scrambled shRNA sequences. This effect was nearly lost in cells infected with the RalBP1 shRNA but not with Sec5 shRNA.

The p27 Ser-10 residue is essential for p27 cytoplasmic mislocalization via the RalBP1 pathway but not for the opposite effect of PLD1

Phosphorylation of p27 on Ser-10 was shown to induce its translocation to and sequestration in the cytoplasm (Rodier *et al.*, 2001; Boehm *et al.*, 2002; Ishida *et al.*, 2002; Besson *et al.*, 2006). Another potentially relevant interaction of p27 is with cyclin E–CDK2, which phosphorylates p27 at Thr-187 (Pagano *et al.*, 1995; Vlach *et al.*, 1997; Montagnoli *et al.*, 1999). We therefore studied the effect of mutating murine p27 residues that inactivate its binding to cyclins (p27(C-)), CDKs (p27(K-)), or both (p27(CK-)), as well as the effect of eliminating the Thr-187 (T187A) or Ser-10 (S10A) phosphorylation site. As shown in Figure 7, the S10A mutation effectively blocked the cytoplasmic mislocalization of the mutated p27 proteins by RalA(Q72L), suggesting that phosphorylation of Ser-10 is essential for its cytoplasmic mislocalization by activated RalA. The p27(CK-) double mutation also had some effect, most likely due to its dual nature (inhibition of binding both to cyclins and CDK).

Because activation of RalBP1 by RalA induces p27 translocation to the cytoplasm (Figures 3 and 4), whereas PLD1 appears to be required for its nuclear localization (Figures 5 and 6), we explored whether the RalBP1 and PLD1 pathways differ in the requirement for Ser-10 on p27. To that end, we investigated the effects of the S10A mutation on the ability of RalA(Q72L), its effector mutants (RalA(Q72L/D49N) and RalA(Q72L/ΔN11), which are defective in RalBP1 or PLD1 binding, respectively), or DN-PLD1 to mislocalize GFP-p27. The results (Figure 8) demonstrate that whereas the S10A mutation blocked the mislocalization of p27 by RalA(Q72L/D49N) as effectively as by RalA(Q72L), it did not impair the ability of DN-PLD1 or RalA(Q72L/ΔN11) (the double mutant defective in PLD1 binding) to mislocalize GFP-p27. These results suggest that the mechanism by which RalBP1 mediates p27 cytoplasmic mislocalization involves phosphorylation of p27 on Ser-10. Several kinases were reported to phosphorylate this Ser residue; an obvious candidate is Akt, whose activity was recently reported to be reduced after RalBP1 knockdown (Leake *et al.*, 2012). We therefore examined the effects of LY294002 (PI3K inhibitor) and MK-2206 (Akt inhibitor; Martina *et al.*, 2012) on the ability of RalA(Q72L) and the constitutively active RalBP1-RalA chimera to induce p27 cytoplasmic mislocalization. The results (Figure 9) demonstrate that both inhibitors abrogate the Ral-mediated effects, suggesting that the mechanisms by which RalBP1 induces Ser-10 phosphorylation on p27 and its accumulation in the cytoplasm proceeds via activation of Akt. Down-regulation of the RalBP1 effectors Cdc42 and Rac does not appear to be involved since inhibition of Rac by 50 μM NSC 23766 (Sanz-Moreno *et al.*, 2008) and of Cdc42 by 10 μM secramine A (Pelish *et al.*, 2006; Xu *et al.*, 2006) after the same protocol described in Figure 9 for PI3K and Akt inhibitors did not induce any noticeable effects on p27 mislocalization.

On the other hand, the opposing PLD1-induced contribution to p27 nuclear localization is mediated by a distinct mechanism, which is independent of Ser-10 phosphorylation. Of note, the ability of RalA(Q72L/ΔN11) to translocate p27(S10A) to the cytoplasm

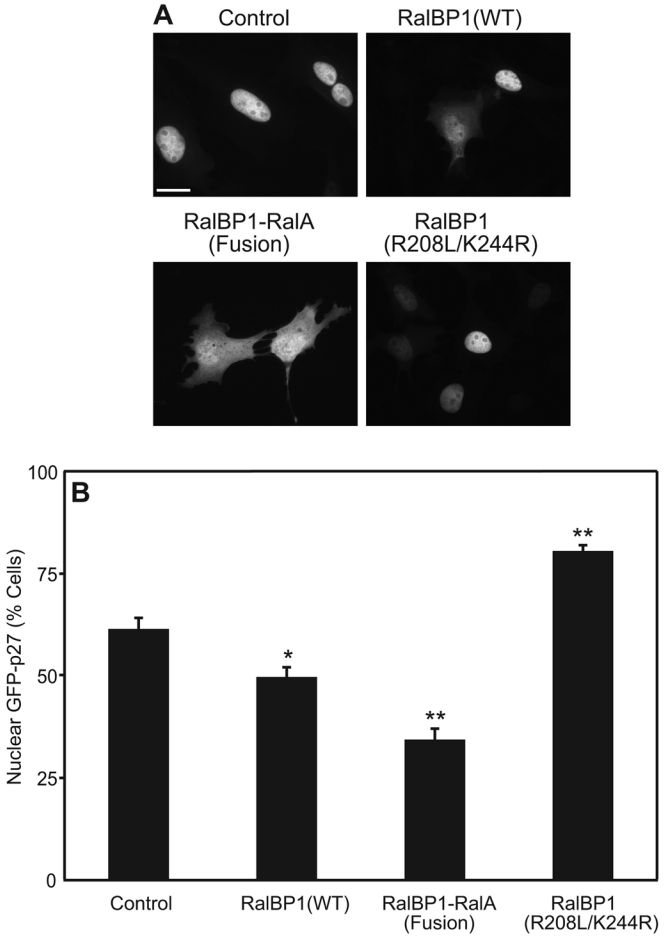

FIGURE 4: Constitutively active RalBP1-RalA fusion protein, but not GAP-dead RalBP1, induces cytoplasmic mislocalization of p27. Mv1Lu cells were cotransfected by murine GFP-p27 together with an excess of the indicated vectors (control, empty vector) as described under *Materials and Methods* and in Figure 2. At 24 h posttransfection, cells were fixed and imaged (see *Materials and Methods*). (A) Typical images of murine GFP-p27 localization. Bar, 20 μm. (B) Quantification of GFP-p27 localization. Bars, means ± SEM of 5–8 samples in each case, scoring 100 transfected cells per sample. Asterisks indicate significant differences from the control (**$p < 2 \times 10^{-4}$; *$p < 0.02$; Student's *t* test). Mainly nuclear GFP-p27 localization is evident in the control, and even more so in cells transfected with the GAP-dead RalBP1(R208L/K244R) mutant. In contrast, the constitutively active RalBP1-RalA fusion protein was highly effective in inducing GFP-p27 cytoplasmic localization, whereas RalBP1(WT) had only a mild effect.

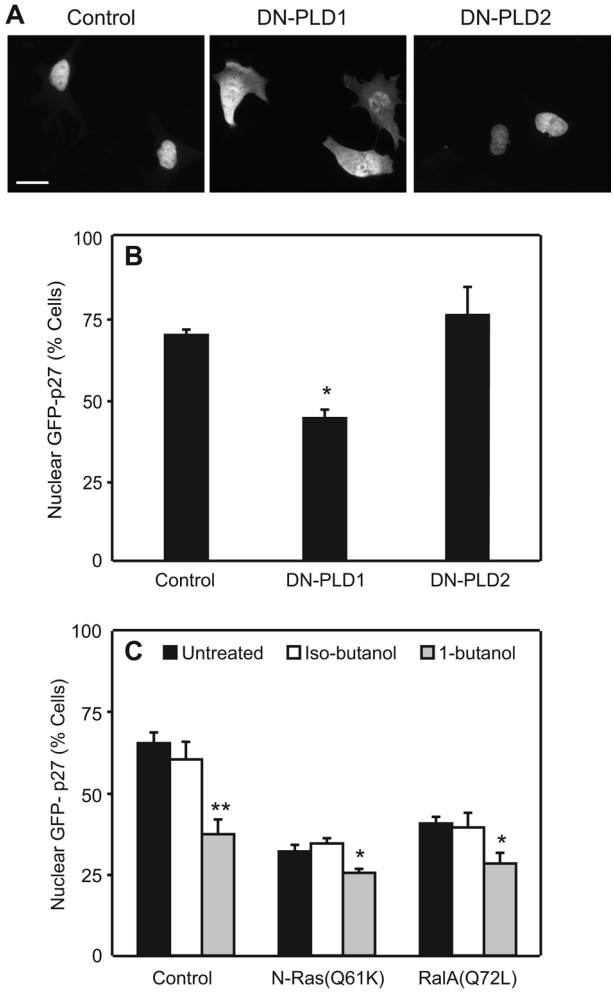

FIGURE 5: Inhibition of PLD by DN-PLD1 or 1-butanol induces p27 cytoplasmic localization. Mv1Lu cells were either cotransfected (as in Figure 2) with murine GFP-p27 together with an excess of empty vector (control), DN-PLD1, DN-PLD2, N-Ras(Q61K), or RalA(Q72L). (A) Typical images of murine GFP-p27 in cells expressing DN-PLD1 or DN-PLD2. At 24 h posttransfection, the cells were fixed and imaged as described under *Materials and Methods*. Bar, 20 μm. (B) Quantification of the effects of DN-PLD1 or DN-PLD2 on GFP-p27 localization. Bars, mean ± SEM of four to nine samples in each case, scoring 100 transfected cells per sample. Asterisks denote significant differences from the control (**$P < 2 \times 10^{-5}$; Student's *t* test). Mainly nuclear localization is evident for the control and for DN-PLD2. In contrast, DN-PLD1 was highly effective in sequestering GFP-p27 in the cytoplasm. (C) Inhibition of PLD by 1-butanol induces p27 cytoplasmic mislocalization. At 24 h posttransfection, the cells were incubated for another 24 h in fresh medium containing 1% (vol/vol) 1-butanol or iso-butanol, fixed, and imaged as described. Bars, means ± SEM of four experiments, scoring 100 transfected cells per sample. Asterisks indicate a significant difference from the untreated cells of each set of similarly transfected cells (**$p < 0.006$; *$p < 0.02$).

demonstrates that the effect of this RalA mutant stems at least in part from its inability to bind PLD1, as inhibition of the latter pathway appears to counteract its contribution to p27 nuclear localization independent of Ser-10. Importantly, the cytoplasmic sequestration of p27(S10A) by RalA(Q72L/ΔN11) links the effects of PLD1 on p27 localization with RalA downstream signaling. The mechanism of the latter effect remains to be explored.

RalA(Q72L) blocks TGF-β1 growth arrest without interfering with TGF-β–induced Smad nuclear translocation

We previously demonstrated that activation of RalA by constitutively active N-Ras induces cytoplasmic accumulation of p27, thereby disrupting TGF-β–mediated growth arrest in Mv1Lu cells (Liu *et al.*, 2000; Kfir *et al.*, 2005). The interference of the Ral pathway with the antiproliferative effect of TGF-β in these cells (used also in the present study) occurred at the level of p27 localization, as the TGF-β signaling events upstream of p27 (including Smad nuclear translocation and transcriptional activation) were unaffected (Liu *et al.*, 2000). Therefore the physiological relevance of the Ral-mediated cytoplasmic accumulation of p27 may be demonstrated by its ability to disrupt TGF-β growth arrest. To explore whether the ability of constitutively active RalA to mislocalize p27 correlates with disruption of

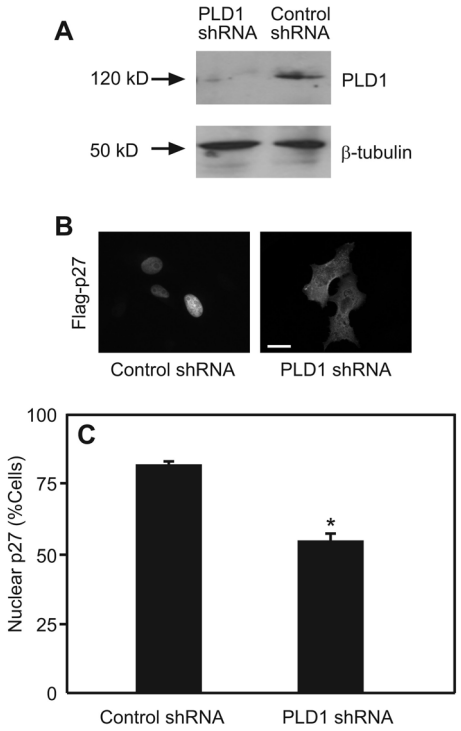

FIGURE 6: Silencing PLD1 expression leads to p27 cytoplasmic localization. A549 cells stably expressing PLD1 shRNA or luciferase shRNA (control) were prepared as described under *Materials and Methods*. (A) Western blotting of human PLD1 (see *Materials and Methods*) shows a strong reduction of endogenous PLD1. The reduction (± SEM; normalized to the loading control) was by 80 ± 11% ($n = 3$). (B) Typical images of Flag-p27 localization. The cells were transfected with Flag-p27, fixed/permeabilized, and labeled by successive incubations with 1) mouse anti-Flag (5 μg/ml), 2) biotin-GαM IgG (5 μg/ml), and 3) Cy3-streptavidin (1.2 μg/ml), followed by fluorescence imaging. Bar, 20 μm. (C) Quantification of Flag-p27 localization. Bars, means ± SEM of three or four experiments, scoring 100 transfected cells per sample. The PLD1 shRNA induced a significant shift of Flag-p27 to the cytoplasm (**$p < 0.003$; Student's *t* test).

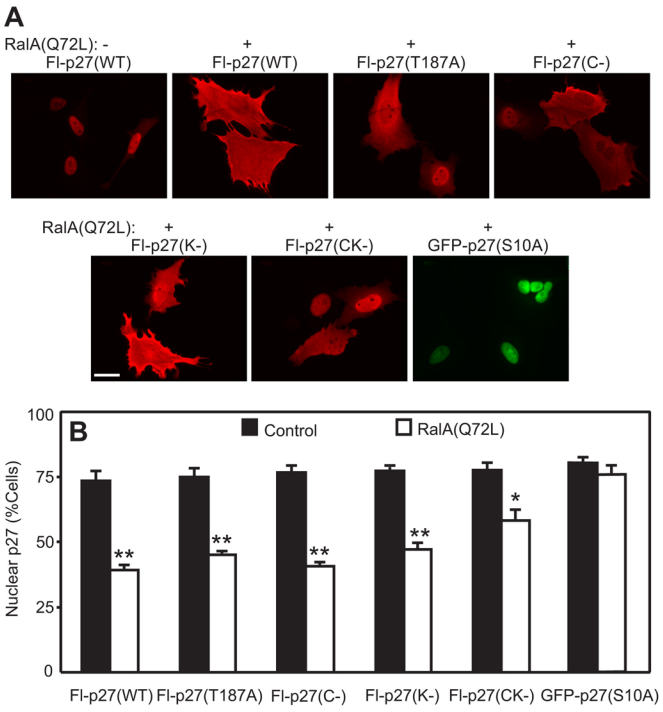

FIGURE 7: Ser-10 on p27 is required for its Ral-mediated accumulation in the cytoplasm. Mv1Lu cells were cotransfected with a vector encoding murine Flag-p27 (Fl-p27) (WT, p27(T187A), p27(C-), p27(K-), p27(CK-)) or GFP-p27(S10A), together with an excess of empty vector (control) or RalA(Q72L). After 24 h, cells were fixed/permeabilized and processed for immunofluorescence as in Figure 6. (A) Typical images of the effects of RalA(Q72L) on the localization of p27 mutants. Bar, 20 μm. (B) Quantification of the localization of GFP-p27. Bars are means ± SEM of four experiments, scoring 100 transfected cells per sample. Asterisks denote significant differences in p27 nuclear localization between cells expressing only the respective p27 mutant (control; black bars) and cells expressing the same p27 construct together with RalA(Q72L) (**$p < 3 \times 10^{-4}$; *$p < 0.004$; Student's *t* test). Only the p27(S10A) mutant was insensitive to RalA(Q72L)-mediated cytoplasmic mislocalization.

TGF-β–induced growth arrest, we measured the effects of RalA(Q72L), RalA(Q72L/D49N), and RalA(Q72L/ΔN11) on the ability of TGF-β1 to inhibit bromodeoxyuridine (BrdU) nuclear incorporation in Mv1Lu cells (Figure 10). Whereas TGF-β1 markedly attenuated BrdU nuclear incorporation in control cells, this effect was completely abolished by RalA(Q72L) and RalA(Q72L/ΔN11). In contrast, RalA(Q72L/D49N), which is defective in binding RalBP1, failed to reverse the effect of TGF-β1 on BrdU incorporation (Figure 10). These results are in full correlation with the effects of the RalA mutants on p27 localization. Of note, the disruption of TGF-β growth inhibition by activated RalA does not arise already at the earlier stage of Smad nuclear translocation, as shown by insensitivity of TGF-β–induced Smad2/3 nuclear translocation to RalA(Q72L) (Figure 11). Together with our earlier demonstration that Ras-mediated activation of the Ral-GEF pathway does not affect TGF-β signaling up to the stage of p27 cellular localization (Liu *et al.*, 2000; Kfir *et al.*, 2005), these findings suggest that activated RalA abrogates TGF-β growth inhibition via RalBP1-mediated p27 cytoplasmic mislocalization.

DISCUSSION

Cytoplasmic translocation of p27 was shown to disrupt normal cell cycle arrest, including TGF-β–mediated growth arrest (Liu *et al.*, 2000; Liang *et al.*, 2002; Shin *et al.*, 2002; Viglietto *et al.*, 2002; Kfir *et al.*, 2005). Moreover, cytoplasmic localization of p27 was reported to promote cell migration (Besson *et al.*, 2004) and to be associated with Ras-dependent lung tumorigenesis in mice (Besson *et al.*, 2006). Of note, activation of the Ral-GEF pathway by oncogenic N-Ras was shown to mislocalize both murine and human p27 from the nucleus to the cytoplasm, compromising the ability of p27 to induce TGF-β–mediated cell cycle arrest (Liu *et al.*, 2000; Kfir *et al.*, 2005). However, the mechanisms by which the multiple signaling pathways downstream of Ral regulate p27 localization remained enigmatic. In the present work, after finding that p27 mislocalization can be induced by activation of either RalA or RalB (Figure 1), we investigated the mechanisms involved using specific RalA and p27 mutants. We show dual effects of RalA signaling on p27 localization, with opposing effects induced by the RalBP1 and PLD1 pathways. Activation of RalBP1 leads to cytoplasmic accumulation of p27 by a mechanism that requires phosphorylation of Ser-10 on p27 by Akt. This pathway appears to operate against a pressure toward nuclear localization of p27 via the PLD1 pathway, which is independent of Ser-10. The disruption of TGF-β growth inhibition after p27 mislocalization by Ral-mediated activation of the RalBP1 pathway attests to the relevance of this phenomenon to TGF-β cellular responses.

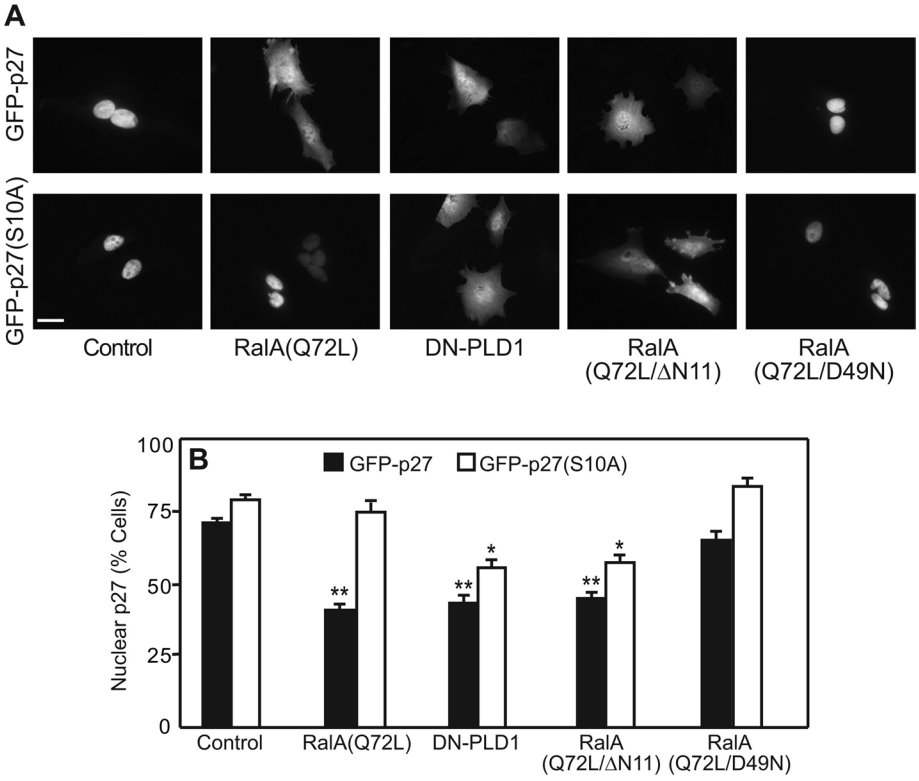

FIGURE 8: The Ser-10 mutation renders p27 insensitive to cytoplasmic mislocalization by the RalBP1 pathway while retaining the response to PLD1. Mv1Lu cells were cotransfected with murine GFP-p27 or GFP-p27(S10A) together with an excess of the indicated vectors (control, empty vector). After 24 h, the cells were fixed and imaged (*Materials and Methods*). (A) Typical images comparing the effects of RalA(Q72L) mutants or DN-PLD1 on the localization of GFP-p27 and GFP-p27(S10A). Bar, 20 μm. (B) Quantification of GFP-p27 and GFP-p27(S10A) localization. Bars, means ± SEM of four to six experiments in each case, scoring 100 transfected cells per sample. Asterisks indicate significant differences from the respective control comparing cells singly expressing GFP-p27 or GFP-p27(S10A) (controls) with cells coexpressing the same p27 construct together with one of the indicated vectors (**$p < 2 \times 10^{-5}$; *$p < 0.01$; Student's *t* test). Only RalA(Q72L/D49N) was unable to mislocalize GFP-p27(WT). On the other hand, GFP-p27(S10A) was shifted to the cytoplasm only by DN-PLD1 or RalA(Q72L/ΔN11).

Ral proteins bind to a limited number of effector proteins, the best documented being RalBP1, exocyst subunits, and PLD1 (Cantor *et al.*, 1995; Luo *et al.*, 1997; Moskalenko *et al.*, 2002, 2003; Feig, 2003; van Dam and Robinson, 2006; Bodemann and White, 2008). The results in Figures 2–4 provide several independent lines of evidence that RalA-mediated p27 cytoplasmic mislocalization proceeds via the RalBP1 pathway: 1) among RalA(Q72L) double mutants defective in either RalBP1, exocyst subunits, or PLD1 binding, only the first two lost the ability to mislocalize p27 (Figure 2), demonstrating that the PLD1 pathway is not required for the effect; 2) shRNA-mediated silencing of RalBP1, but not Sec5, abrogated RalA(Q72L)-mediated p27 mislocalization (Figure 3), implicating RalBP1 in the effect; and 3) expression of constitutively active RalBP1-RalA chimera induced p27 mislocalization, whereas GAP-dead RalBP1 (R208L/K244R) enhanced p27 nuclear localization (Figure 4), indicating that RalBP1 activity is not only required but also sufficient to translocate p27 to the cytoplasm. The identification of the RalBP1 pathway as the one mediating p27 cytoplasmic accumulation is in line with numerous reports on its involvement in cancer development (Singhal *et al.*, 2007; Issaq *et al.*, 2010; Lim *et al.*, 2010; Wu *et al.*, 2010).

The ability of RalA(Q72L/ΔN11) to mislocalize p27 in spite of its defective binding to PLD1 (Figure 2) shows that the latter interaction is dispensable for Ral-mediated p27 cytoplasmic accumulation. However, this does not necessarily mean that PLD is not involved in other aspects of p27 localization. Indeed, DN-PLD1 (but not DN-PLD2) was sufficient to translocate p27 to the cytoplasm (Figure 5), raising the possibility that in unperturbed cells PLD1, which is the isoform that binds Ral (Hammond *et al.*, 1995), contributes to the nuclear localization of p27. This notion is supported by the cytoplasmic accumulation of p27 after either inhibition of PLD activity by 1-butanol or knockdown of PLD1 by shRNA (Figures 5 and 6). Although these results imply that PLD1 contributes to the nuclear localization of p27 under normal conditions, they do not distinguish between Ral-dependent and Ra1-independent effects of PLD1. To address this issue, we took advantage of the finding that p27 cytoplasmic mislocalization by the RalA-RalBP1 axis, but not by DN-PLD1, requires Ser-10 on p27 (Figures 7 and 8). Moreover, we identified Akt as the kinase that mediates the phosphorylation of Ser-10 on p27 after expression of activated Ral or RalBP1 (Figure 9). As shown in Figure 8, an RalA mutant defective in PLD1 binding, RalA(Q72L/ΔN11), is as effective as DN-PLD1 in mediating cytoplasmic accumulation of p27(S10A), suggesting that loss of RalA–PLD1 interactions can lead to p27 mislocalization. Further studies should address the mechanism by which PLD1 and its product, phosphatidic acid, link to p27 localization. Taking these results together, we propose that RalA regulates p27 nuclear/cytoplasmic localization by a dual mechanism, based on balancing two negating pathways: RalBP1-Akt

Because Ral-GEF activation mislocalizes p27 (Kfir *et al.*, 2005) and both RalA and RalB are Ral-GEF substrates, we compared their ability to mislocalize p27. The results in Figure 1 demonstrate that the ability to induce p27 cytoplasmic mislocalization is shared by the two Ral isoforms. This is in line with the involvement of both RalA and RalB in tumorigenicity but also indicates that their distinct contributions to cancer progression (Lim *et al.*, 2005, 2006; Oxford *et al.*, 2005; Rosse *et al.*, 2006; Bodemann and White, 2008; Martin *et al.*, 2011) are not due to different effects on p27 localization. Of interest, the ability of the Ral proteins to mislocalize p27 directly correlates with the extent of their activation (mild vs. strong effects mediated by the WT proteins and Q72L mutants, respectively). This correlation also holds for our earlier studies, in which p27 mislocalization was promoted by activated Ral-GEF but inhibited by DN-RalA (Kfir *et al.*, 2005). In view of the similar effects of RalB and RalA, we chose the latter for further analysis.

Of note, murine p27, which lacks the Thr-157 phosphorylation site, was as sensitive as human p27 to Ral-mediated cytoplasmic accumulation (Figure 1). This finding is in accord with the demonstration that Thr157 is dispensable for p27 mislocalization via the Ras-Ral-GEF axis (Liu *et al.*, 2000; Kfir *et al.*, 2005), ruling out participation of Thr-157 phosphorylation in the process.

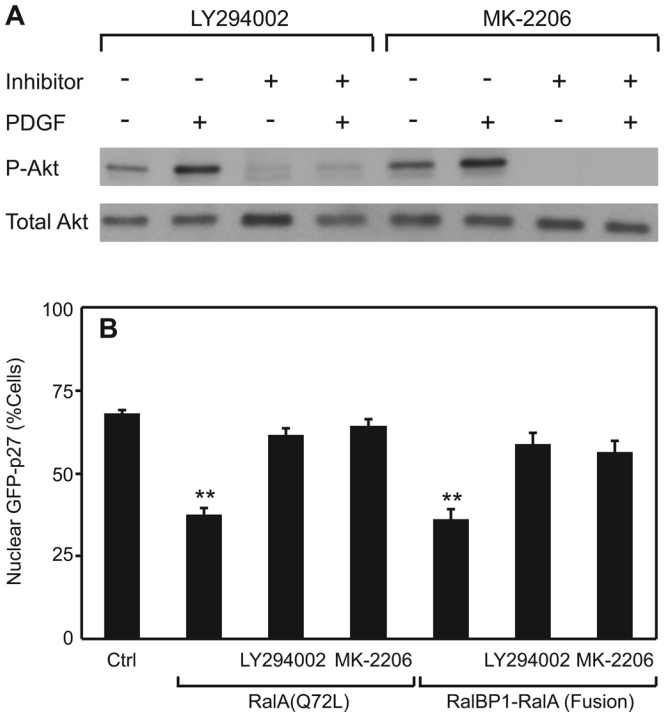

FIGURE 9: Inhibition of Akt and PI3K blocks Ser-10 phosphorylation on p27 and RalBP1-mediated p27 cytoplasmic mislocalization. (A) Pharmacological inhibitors are effective in blocking growth factor stimulation in Mv1Lu cells. After 24 h in serum-free medium, cells were incubated with LY294002 (20 μM) or MK-2206 (1 μM) for 12 h. They were then stimulated (100 ng/ml; 5 min) with PDGF, lysed, and subjected to SDS–PAGE. Electrotransfer was followed by immunoblotting with anti-Akt to determine the total level of Akt or with antibody specific to phospho-Akt (P-Akt) to determine the active form. PDGF induced a 2.0 ± 0.1–fold increase in P-Akt ($n = 3$); the effect was totally blocked by LY294002 or MK-2206. (B) Mv1Lu cells were cotransfected with murine GFP-p27 together with an excess of empty vector (Ctrl), RalA(Q72L), or constitutively active RalBP1-RalA fusion protein. After 24 h the cells were incubated for 16 h with LY294002 (20 μM) or MK-2206 (1 μM), whereas control samples were left untreated. The cells were then fixed and mounted for fluorescence imaging. The graph depicts quantification of GFP-p27 localization, where each bar is the mean ± SEM of four independent experiments, scoring 100 transfected cells per sample. Asterisks indicate significant differences (**$p < 5 \times 10^{-5}$; Student's t test) from the control.

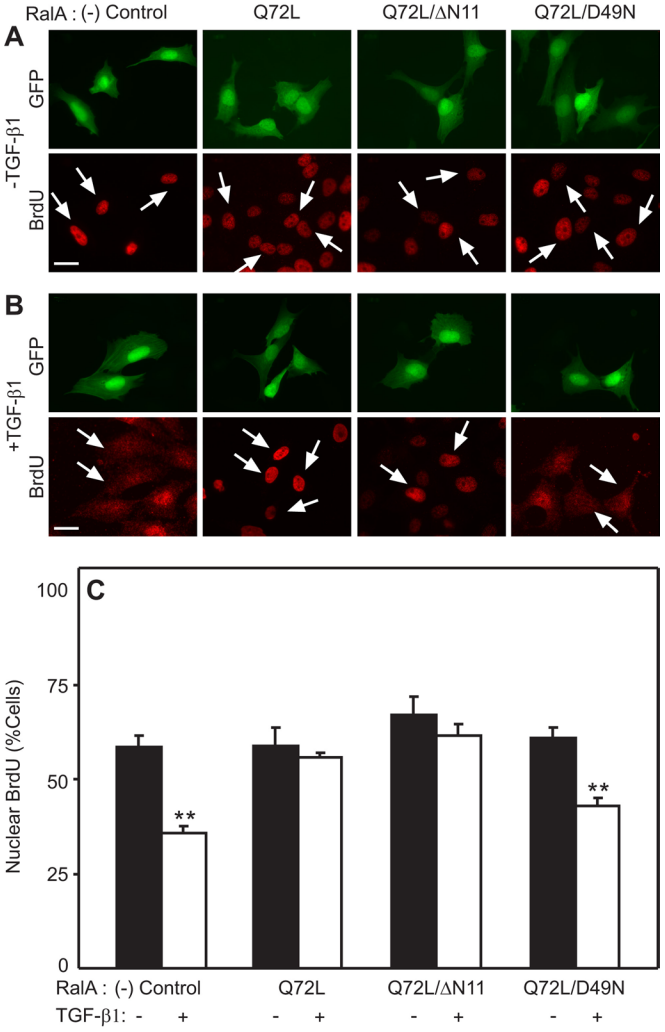

FIGURE 10: Growth arrest by TGF-β1 is disrupted by RalA(Q72L) and RalA(Q72L/ΔN11) but not by RalA(Q72L/D49N). Mv1Lu cells were cotransfected with GFP and an excess of empty vector (control) or the designated constitutively active RalA mutant. After 24 h, cells were incubated without (A) or with (B) TGF-β1 (10 pM; 24 h, 37°C). Incorporation and labeling of BrdU were as described (Kfir *et al.*, 2005; see *Materials and Methods*). (A, B) Typical images of BrdU incorporation. Bar, 20 μm. (C) Quantification of BrdU incorporation. BrdU staining (red) was scored in transfected cells, identified by GFP fluorescence (marked by arrows in the BrdU images). Bars, means ± SEM of four to eight samples in each case, scoring 100 cells per sample. Asterisks indicate significant inhibition of BrdU incorporation by TGF-β1, comparing pairs of samples without and with TGF-β1 (**$p < 0.009$). Constitutively active RalA(Q72L) and RalA(Q72L/ΔN11), but not the RalBP1-defective RalA(Q72L/D49N), completely abrogated the ability of TGF-β1 to inhibit BrdU incorporation.

(mediating cytoplasmic accumulation) and PLD1 (favoring nuclear p27 localization). Of note, PLD1 binding to RalA is constitutive and does not depend on nucleotide binding to RalA (Feig, 2003; van Dam and Robinson, 2006), enabling a basal pressure via the Ral-PLD1 pathway toward nuclear localization of p27. On the other hand, RalBP1 binds only to Ral-GTP; thus the RalBP1 pathway downstream of RalA becomes operative only after RalA activation (Feig, 2003; van Dam and Robinson, 2006), overcoming the opposite drive of the PLD1 pathway and leading to translocation of p27 to the cytoplasm. According to this model, it is expected that overexpression of active RalBP1 would induce p27 cytoplasmic mislocalization by itself; this indeed is the case, as expression of constitutively active RalBP1-RalA fusion protein mediates p27 mislocalization, whereas overexpression of GAP-dead RalBP1 enhances nuclear p27 (Figure 4). Finally, the physiological relevance of Ral-mediated cytoplasmic mislocalization of p27 is underscored by the resulting disruption of TGF-β–mediated cell cycle arrest and growth inhibition (Figures 10 and 11). This phenomenon might contribute to aberrant TGF-β signaling in the context of chronic Ral activation, in line with reports on the loss of TGF-β growth inhibition and enhanced metastasis in epithelial tumor cells after Ras constitutive activation or overactivation (Oft *et al.*, 1996, 2002; Lehmann *et al.*, 2000; Liu *et al.*, 2000; Derynck *et al.*, 2001; Guo and Wang, 2009).

MATERIALS AND METHODS

Reagents

Recombinant TGF-β1 was obtained from PeproTech (Rocky Hill, NJ). Rabbit immunoglobulin Gs (IgGs) against Smad3 (reactive with

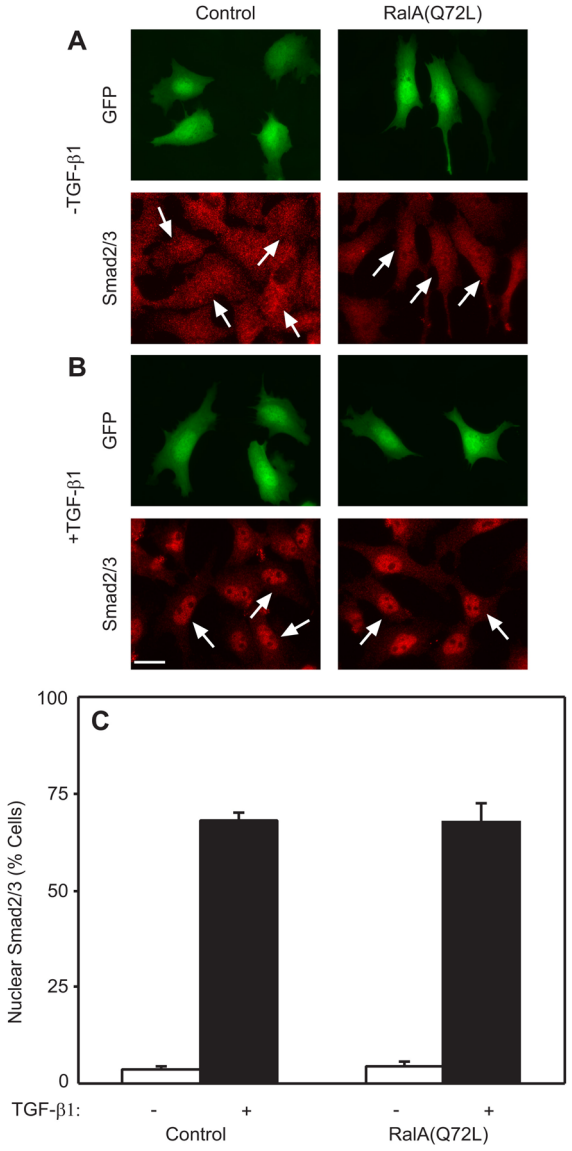

FIGURE 11: RalA(Q72L) does not inhibit Smad2/3 nuclear translocation in response to TGF-β1. Mv1Lu cells were cotransfected with GFP together with an excess of RalA(Q72L) or empty vector (control). After 24 h, they were incubated without (A) or with (B) TGF-β1 (100 pM, 20 min, 37°C), fixed/permeabilized, and processed for immunofluorescence (see *Materials and Methods*). The arrows in the Smad2/3 images indicate transfected cells, identified by GFP fluorescence. Bar, 20 μm. (C) Quantification of Smad2/3 localization. Bars, means ± SEM of three samples in each case, scoring 100 cells per sample. TGF-β1 induced strong and similar accumulation of Smad2/3 in control cells and in cells expressing RalA(Q72L) ($p > 0.2$), comparing TGF-β–stimulated control cells with RalA(Q72L)-expressing cells.

Smad3 and Smad2; sc-8332) or human p27 (sc-528) were from Santa Cruz Biotechnology (Santa Cruz, CA). Goat γ-globulin, affinity-purified biotinylated IgGs (goat anti-rabbit [GαR], goat anti-mouse [GαM], and rabbit anti-mouse), Cy3-streptavidin, peroxidase-GαM, and peroxidase-GαR IgGs were from Jackson ImmunoResearch (West Grove, PA). Mouse anti–β-actin was from MP Biomedicals (Solon, OH). The BrdU labeling kit with anti-BrdU antibodies (18-0103) was from Invitrogen-Zymed Laboratories (San Francisco, CA). Mouse anti-RalBP1 was obtained from Abnova (Taipei City, Taiwan). Mouse monoclonal anti-Flag (M2), affinity-purified rabbit anti human PLD1 (PC-specific), mouse anti–β-tubulin, 1-butanol, puromycin, and polybrene were from Sigma-Aldrich (St. Louis, MO). Rabbit antibodies against Akt or phospho-Akt (Ser-473) were from Cell Signaling (Beverly, MA). Iso-butanol (2-methyl-1-propanol) was from Merck (Darmstadt, Germany). Affinity-purified rabbit IgG against the influenza hemagglutinin (HA) epitope tag (anti-HA) was from Bethyl Laboratories (Montgomery, TX). G418 was purchased from Calbiochem (La Jolla, CA). Recombinant platelet-derived growth factor (PDGF)-BB was from R&D Systems (Minneapolis, MN). The PI3K inhibitor LY294002 was purchased from Calbiochem, the Akt inhibitor MK-2206 from Selleck Chemicals (Munich, Germany), and the Rac inhibitor NSC 23766 from Tocris (Ellisville, MO). The Cdc42 inhibitor secramine A (Pelish *et al.*, 2006; Xu *et al.*, 2006), synthesized by B. Xu and G. B. Hammond, was donated by T. Kirchhausen (Harvard Medical School, Boston, MA) and G. B. Hammond (University of Louisville, Louisville, KY).

Plasmids

Constitutively active human N-Ras(Q61K) in pcDNA3 (Wolfman *et al.*, 2002) was a gift from C. J. Der and A. D. Cox (University of North Carolina, Chapel Hill, NC). WT human RalA and RalB, their constitutively active mutants RalA(Q72L) and RalB(Q72L) (Emkey *et al.*, 1991), and DN RalA(S28N) (Goi *et al.*, 1999) in pBABE-puro were a gift from C. M. Counter (Duke University Medical Center, Durham, NC; Lim *et al.*, 2005). Double mutants of RalA(Q72L) deficient in activating one of the Ral-activated pathways (RalBP1, the exocyst, or PLD1) were donated by C. M. Counter (Lim *et al.*, 2005). These include 1) RalA(Q72L/D49N), which fails to bind RalBP1 (Cantor *et al.*, 1995); 2) RalA(Q72L/D49E), defective in binding Sec5 and Exo84 (Moskalenko *et al.*, 2002, 2003); and 3) RalA(Q72L/ΔN11), which lacks the 11 N-terminal amino acids and is defective in PLD1 binding (Jiang *et al.*, 1995). pCS2 vectors encoding murine Flag-p27, its T187A mutant lacking the cyclin E–CDK2 phosphorylation site, and Flag-p27 mutants defective in cyclin or CDK binding (Ungermannova *et al.*, 2005) were a gift from X. Liu (University of Colorado, Boulder, CO). The last-named mutants (described originally in Vlach *et al.*, 1997) are defective in binding cyclins (R30A/L32A, designated p27(C-)), CDKs (F62A/F64A, designated p27(K-)), or both (p27(CK-) mutant). Human HA-p27 in pcDNA3 (Rodier *et al.*, 2001) was donated by M. Pagano (New York University School of Medicine, New York, NY). Green fluorescent protein (GFP)–tagged murine p27 in pEGFP-C1 was as described (Kfir *et al.*, 2005). This vector served as template to generate GFP-p27(S10A) (lacking the Ser-10 phosphorylation site) by site-directed mutagenesis (QuikChange; Stratagene, Santa Clara, CA), using primers 5′-AGAGTGTCTAACGGG**GCC**CCG-AGCCTG-GAGCG-3′ (forward) and 5′-CGCTCCAGGCTCGG**GGC**CCCGTTA-GACACTCT-3′ (reverse) for the S10A mutation (bold letters indicate the Ala codon). Inactive, dominant-negative human PLD1b(K898R) (DN-PLD1) and murine PLD2(K758R) (DN-PLD2) in pCGN (Sung *et al.*, 1997; Du *et al.*, 2004) were a gift from M. Frohman (SUNY, School of Medicine, Stony Brook, NY). Expression vectors for myc-tagged human RalBP1 (Lim *et al.*, 2010) in pcDNA3.1 and myc-RalBP1 fused with the last 30 amino acids of RalA (RalBP1-RalA, constitutively active due to membrane anchorage by the RalA sequence) in pWZL-blast (Kashatus *et al.*, 2011) were generously provided by C. M. Counter, as well as the GAP-dead mutant RalBP1(R208L/K244R) in pcDNA3.1, generated by introducing the mutations described for *Xenopus* RalBP1 (Boissel *et al.*, 2007) into the cDNA encoding the human protein. pCMV-Gag-Pol encoding the structure proteins of the Moloney murine leukemia retrovirus and the pMD2G vector encoding the VSV G envelope protein

were donated by Y. Kloog (Tel Aviv University, Tel Aviv, Israel; Shalom-Feuerstein *et al.*, 2008). shRNA to human RalBP1 (5′-GTAGAGAGGACCATGATGT-3′), human Sec5 (5′-CGGCAGAATGGATGTCTGC-3′), and their scrambled versions, all in pSuperRetro-puro (Issaq *et al.*, 2010; Lim *et al.*, 2010), were donated by C. M. Counter. Both shRNA-targeted small interfering RNA (siRNA) sequences are identical in human and murine RalBP1 or Sec5. Human PLD1 was silenced using a pEGFP-N2 shRNA plasmid (thus expressing enhanced GFP) containing an H1 promoter, followed by a siRNA sequence targeting human PLD1 (nucleotides 547–565; 5′-CTGGAAGATTACTTGACAA-3′; Zeniou-Meyer *et al.*, 2007) or an unrelated luciferase sequence donated by U. Ashery (Tel Aviv University, Tel Aviv, Israel).

Tissue culture and transfection

Mv1Lu, Cos7, HEK 293T, and A549 cells (American Type Culture Collection, Manassas, VA) were grown as described (Liu *et al.*, 2000; Viglietto *et al.*, 2002; Besson *et al.*, 2004; Shapira *et al.*, 2012). For immunofluorescence and BrdU incorporation assays, subconfluent Mv1Lu or Cos7 cells plated on glass coverslips in six-well plates were transfected with 2 μg of DNA (cotransfected plasmids were supplemented to 2 μg of DNA with empty vector where needed) using TransIT-LT1 Mir2300 (Mirus, Madison, WI). A549 cells were grown on glass coverslips as described (Besson *et al.*, 2004), transfected with 2 μg of DNA by Lipofectamine 2000 (Invitrogen, Carlsbad, CA), and processed for immunofluorescence 24 h later.

Retroviral infection

HEK 293T cells in 10-cm dishes were cotransfected twice (at a 24-h interval) by the calcium phosphate method with 10 μg each of pSuperRetro-puro shRNA against RalBP1 or Sec5, together with pMD2G and pCMV-Gag-Pol. After another 24 h, the cell supernatant was filtered through a 0.45-μm filter, complemented with 2 ml of fresh complete media and 10 μl of polybrene (from 4 mg/ml stock), and placed onto Mv1Lu cells grown in 10-cm dishes, replacing the growth medium. The transfected HEK 293T cells were replenished with 10 ml of fresh medium; after 24 h, the medium was filtered, and the procedure with the Mv1Lu cells was repeated for a second cycle of infection (24 h). The Mv1Lu cells were allowed to recover for 24 h in fresh medium, which was then replaced by medium containing 2 μg/ml puromycin for selection (2 wk). Cells were kept under selection at all times.

Stable transfection of A549 cells with PLD1 shRNA

Nearly confluent A549 cells in 10-cm dishes were transfected with 10 μg of DNA (PLD1 shRNA or luciferase shRNA in pEGFP-N2) by Lipofectamine 2000 (Invitrogen) as described under *Tissue culture and transfection*. At 72 h posttransfection, cells were selected in growth medium containing 600 μg/ml G418 (2 wk). GFP-expressing cell populations were sorted by a fluorescence-activated cell sorter (FACSAria; BD Biosciences, San Diego, CA). The GFP-expressing cells were pulled and kept under G418 selection.

Immunofluorescence microscopy

Cells grown and transfected as described under *Tissue culture and transfection* were subjected (or not) to various treatments (1-butanol, TGF-β1 stimulation, BrdU incorporation) as detailed in the specific figure legends. They were then fixed with 4% paraformaldehyde and permeabilized with Triton X-100 as described (Kfir *et al.*, 2005) and stained with 4′,6-diamidino-2-phenylindole (DAPI). After blocking (30 min) with 200 μg/ml goat γ-globulin in Hanks balanced salt solution containing 20 mM 4-(2-hydroxyethyl)-1-piperazineethanesulfonic acid (pH 7.2) and 2% bovine serum albumin, the cells were labeled successively (45 min, 22°C for each antibody) with various antibodies (see figure legends) in the same buffer, with three extensive washes between steps. Cells were mounted with fluorescence mounting medium (Golden Bridge International, Mukilteo, WA), and fluorescence digital images were captured by a charged-coupled device camera (CoolSNAP HQ-M; Photometrics, Tucson, AZ) mounted on an AxioImager D.1 microscope (Carl Zeiss Microimaging, Jena, Germany) with a 63×/1.4 numerical aperture objective. Images were imported into and analyzed by SlideBook (Intelligent Imaging Innovations, Denver, CO). The cells were intensity based segmented with the DAPI channel to mark the nucleus. The fluorescence of GFP-p27 (or of p27 labeled with fluorescent antibodies) in the nucleus was divided by the total fluorescence of p27 (nucleus and cytoplasm) to obtain the percentage of nuclear p27. When this value was 60% or higher, the cells were defined as showing predominantly nuclear p27 localization, whereas a value of 25% or less was taken to represent a mainly cytoplasmic distribution. More than 95% of the cells could be sorted by these definitions.

Smad2/3 nuclear translocation assay

Mv1Lu cells were cotransfected with a transfection marker (pEGFP) and a sixfold excess of RalA(Q72L) or empty vector (control). After 24 h, cells were stimulated (or not) with 100 pM TGF-β1 (20 min), fixed/permeabilized, and blocked with goat γ-globulin (200 μg/ml, 30 min, 22°C; see *Immunofluorescence microscopy*). They were then labeled successively by 1) rabbit IgG reactive with Smad2/3 (5 μg/ml); 2) biotin-GαR IgG (5 μg/ml); and 3) Cy3-streptavidin (1.2 μg/ml). Cells were mounted and imaged as described under *Immunofluorescence microscopy*.

BrdU incorporation

Mv1Lu cells were seeded for 1 d on glass coverslips in six-well dishes (65,000 cells/dish) and cotransfected with a transfection marker (pEGFP) and a sixfold excess of empty vector, RalA(Q72L) or one of the RalA double mutants in pBABE-puro. After 24 h, the cells were incubated with or without TGFβ-1 (10 pM, 24 h, 37°C), followed by addition of BrdU (1:100 dilution from the labeling kit) for another 24 h. They were then fixed with 4% paraformaldehyde, permeabilized with Triton X-100, and subjected to BrdU immunostaining following the protocol described previously (Kfir *et al.*, 2005). This protocol results in BrdU labeled by Cy3-streptavidin (red fluorescence). Transfected cells were identified by GFP fluorescence and scored for nuclear BrdU labeling.

Real-time reverse transcriptase-PCR

To measure mRNA expression levels of exogenously expressed RalA or RalB constructs, Mv1Lu were transfected as described under *Tissue culture and transfection*. Total RNA was isolated from the cells by EZ-RNA (Biological Industries, Kibbutz Beit HaEmek, Israel), followed by reverse transcription using Verso RT-PCR Kit (Thermo Scientific, Waltham, MA). Real-time reverse transcriptase (RT)–PCR analysis of the mRNA levels of the transfected Ral constructs relative to 18S RNA was done in triplicate using KAPA SYBR FAST ABI Prism qPCR kit (Kapa Biosystems, Woburn, MA) with ABI Prism 7300 (Applied Biosystems, Foster City, CA). Gene expression values were calculated based on the comparative threshold cycle method (Livak and Schmittgen, 2001). To measure the mRNA levels of the transfected Ral-encoding plasmids (without interference by endogenous Ral mRNA), real-time RT-PCR primers were designed such that the forward primer localized to the coding sequence of RalA or RalB and the reverse primer localized to the region preceding the poly(A)

sequence of the pBABE-puro plasmid. These sequences were 5′-GAGGCAAAAAACAGAGCTGAGCAG-3′ (forward for RalA) or 5′-AGAACAAAGAAGATGTCAGAA-3′ (forward for RalB) and 5′-CTGACACACATTCCACAGGGTCGA-3′ (reverse). For 18S RNA the sequences were 5′-CGGCTACCACATCCAAGGAAGG-3′ (forward) and 5′-CGCTCCCAAGATCCAACTAC-3′ (reverse).

To measure the efficiency of shRNA-mediated knockdown of Sec5, Mv1Lu cells were infected with retroviruses encoding Sec5 shRNA or scrambled control and grown under puromycin selection as described under *Retroviral infection*. Total RNA was isolated from the cells, followed by reverse transcription as described. Real-time RT-PCR analysis of total Sec5 mRNA relative to 18S RNA was done in triplicate, followed by calculation of gene expression values as described. Because the sequence of mink Sec5 is not available, the real-time RT-PCR Sec5 primers were chosen for sequences conserved between mouse and human Sec5. These sequences were 5′-GGGACAAGCCAAAAATGACAAAGG-3′ (forward) and 5′-CTCACTTGTAAAATCAGCAC-3′ (reverse). For 18S RNA the sequences were as described.

Immunoblotting

Mv1Lu cells (untreated, infected with shRNA vectors, or sorted by flow cytometry) were subjected to lysis, SDS–PAGE, and immunoblotting exactly as described previously (Kfir *et al.*, 2005), with 20 µg of protein loaded per lane. Blots were probed with anti-RalBP1 (1:1000, 12 h, 4°C), followed by peroxidase-GαM (1:5000, 1 h, 22°C), anti-PLD1 (1:1000, 12 h, 4°C) followed by peroxidase-GαR (1:1000, 1 h, 22°C), or anti-phospho-Akt (1:000, 12 h, 4°C) followed by peroxidase-GαR (1:5000, 1 h, 22°C). For loading controls, the blots were acid stripped (Kfir *et al.*, 2005) and reprobed with anti–β-actin (1:10,000), anti–β-tubulin (1:1000), or anti-Akt (1:4000), followed by peroxidase-coupled secondary antibody (1:10,000). The bands were visualized by enhanced chemiluminescence (Amersham, Piscataway, NJ), and quantified by densitometry (EZQuant-Gel2.2; EZQuant, Tel Aviv, Israel).

ACKNOWLEDGMENTS

We thank U. Ashery, C. M. Counter, A. D. Cox, C. J. Der, M. Frohman, Y. Kloog, X. Liu, and M. Pagano for plasmids and T. Kirchhausen and G. B. Hammond for secramine A. We are grateful to C. M. Counter for advice. This work was supported by grants from the Israel Science Foundation (158/09) and the Israel Cancer Research Fund (to Y.I.H.). Y.I.H. is an incumbent of the Zalman Weinberg Chair in Cell Biology.

REFERENCES

Besson A, Dowdy SF, Roberts JM (2008). CDK inhibitors: cell cycle regulators and beyond. Dev Cell 14, 159–169.

Besson A, Gurian-West M, Chen X, Kelly-Spratt KS, Kemp CJ, Roberts JM (2006). A pathway in quiescent cells that controls $p27^{Kip1}$ stability, subcellular localization, and tumor suppression. Genes Dev 20, 47–64.

Besson A, Gurian-West M, Schmidt A, Hall A, Roberts JM (2004). $p27^{Kip1}$ modulates cell migration through the regulation of RhoA activation. Genes Dev 18, 862–876.

Bi K, Roth MG, Ktistakis NT (1997). Phosphatidic acid formation by phospholipase D is required for transport from the endoplasmic reticulum to the Golgi complex. Curr Biol 7, 301–307.

Bloom J, Pagano M (2003). Deregulated degradation of the cdk inhibitor p27 and malignant transformation. Semin Cancer Biol 13, 41–47.

Bodemann BO, White MA (2008). Ral GTPases and cancer: linchpin support of the tumorigenic platform. Nat Rev Cancer 8, 133–140.

Boehm M, Yoshimoto T, Crook MF, Nallamshetty S, True A, Nabel GJ, Nabel EG (2002). A growth factor-dependent nuclear kinase phosphorylates $p27^{Kip1}$ and regulates cell cycle progression. EMBO J 21, 3390–3401.

Boissel L, Houssin N, Chikh A, Rynditch A, Van Hove L, Moreau J (2007). Recruitment of Cdc42 through the GAP domain of RLIP participates in remodeling of the actin cytoskeleton and is involved in Xenopus gastrulation. Dev Biol 312, 331–343.

Bos JL (1989). Ras oncogenes in human cancer: a review. Cancer Res 49, 4682–4689.

Boucrot E, Saffarian S, Massol R, Kirchhausen T, Ehrlich M (2006). Role of lipids and actin in the formation of clathrin-coated pits. Exp Cell Res 312, 4036–4048.

Cantor SB, Urano T, Feig LA (1995). Identification and characterization of Ral-binding protein 1, a potential downstream target of Ral GTPases. Mol Cell Biol 15, 4578–4584.

Chien Y, White MA (2003). RAL GTPases are linchpin modulators of human tumour-cell proliferation and survival. EMBO Rep 4, 800–806.

Chu IM, Hengst L, Slingerland JM (2008). The Cdk inhibitor p27 in human cancer: prognostic potential and relevance to anticancer therapy. Nat Rev Cancer 8, 253–267.

Datto MB, Li Y, Panus JF, Howe DJ, Xiong Y, Wang XF (1995). Transforming growth factor β induces the cyclin-dependent kinase inhibitor p21 through a p53-independent mechanism. Proc Natl Acad Sci USA 92, 5545–5549.

Derynck R, Akhurst RJ, Balmain A (2001). TGF-β signaling in tumor suppression and cancer progression. Nat Genet 29, 117–129.

Du G, Huang P, Liang BT, Frohman MA (2004). Phospholipase D2 localizes to the plasma membrane and regulates angiotensin II receptor endocytosis. Mol Biol Cell 15, 1024–1030.

Emkey R, Freedman S, Feig LA (1991). Characterization of a GTPase-activating protein for the Ras-related Ral protein. J Biol Chem 266, 9703–9706.

Ewen ME, Sluss HK, Whitehouse LL, Livingston DM (1993). TGFβ inhibition of Cdk4 synthesis is linked to cell cycle arrest. Cell 74, 1009–1020.

Feig LA (2003). Ral-GTPases: approaching their 15 minutes of fame. Trends Cell Biol 13, 419–425.

Frohman MA, Sung TC, Morris AJ (1999). Mammalian phospholipase D structure and regulation. Biochim Biophys Acta 1439, 175–186.

Goi T, Rusanescu G, Urano T, Feig LA (1999). Ral-specific guanine nucleotide exchange factor activity opposes other Ras effectors in PC12 cells by inhibiting neurite outgrowth. Mol Cell Biol 19, 1731–1741.

Guo X, Wang XF (2009). Signaling cross-talk between TGF-β/BMP and other pathways. Cell Res 19, 71–88.

Hammond SM, Altshuller YM, Sung TC, Rudge SA, Rose K, Engebrecht J, Morris AJ, Frohman MA (1995). Human ADP-ribosylation factor-activated phosphatidylcholine-specific phospholipase D defines a new and highly conserved gene family. J Biol Chem 270, 29640–29643.

Hannon GJ, Beach D (1994). $p15^{INK4B}$ is a potential effector of TGF-β-induced cell cycle arrest. Nature 371, 257–261.

Harbour JW, Luo RX, Dei Santi A, Postigo AA, Dean DC (1999). Cdk phosphorylation triggers sequential intramolecular interactions that progressively block Rb functions as cells move through G1. Cell 98, 859–869.

Hu PP, Datto MB, Wang XF (1998). Molecular mechanisms of transforming growth factor-β signaling. Endocr Rev 19, 349–363.

Iavarone A, Massague J (1997). Repression of the CDK activator Cdc25A and cell-cycle arrest by cytokine TGF-β in cells lacking the CDK inhibitor p15. Nature 387, 417–422.

Ishida N, Hara T, Kamura T, Yoshida M, Nakayama K, Nakayama KI (2002). Phosphorylation of $p27^{Kip1}$ on serine 10 is required for its binding to CRM1 and nuclear export. J Biol Chem 277, 14355–14358.

Issaq SH, Lim KH, Counter CM (2010). Sec5 and Exo84 foster oncogenic ras-mediated tumorigenesis. Mol Cancer Res 8, 223–231.

Jiang H, Lu Z, Luo JQ, Wolfman A, Foster DA (1995). Ras mediates the activation of phospholipase D by v-Src. J Biol Chem 270, 6006–6009.

Kashatus DF, Lim KH, Brady DC, Pershing NL, Cox AD, Counter CM (2011). RalA and RalBP1 regulate mitochondrial fission at mitosis. Nat Cell Biol 13, 1108–1115.

Kfir S, Ehrlich M, Goldshmid A, Liu X, Kloog Y, Henis YI (2005). Pathway- and expression level-dependent effects of oncogenic N-Ras: $p27^{Kip1}$ mislocalization by the Ral-GEF pathway and Erk-mediated interference with Smad signaling. Mol Cell Biol 25, 8239–8250.

Klein J (2005). Functions and pathophysiological roles of phospholipase D in the brain. J Neurochem 94, 1473–1487.

Leake K, Singhal J, Nagaprashantha LD, Awasthi S, Singhal SS (2012). RLIP76 regulates PI3K/Akt signaling and chemo-radiotherapy resistance in pancreatic cancer. PLoS One 7, e34582.

Lehmann K, Janda E, Pierreux CE, Rytomaa M, Schulze A, McMahon M, Hill CS, Beug H, Downward J (2000). Raf induces TGFβ production while blocking its apoptotic but not invasive responses: a mechanism leading to increased malignancy in epithelial cells. Genes Dev 14, 2610–2622.

Liang J *et al.* (2002). PKB/Akt phosphorylates p27, impairs nuclear import of p27 and opposes p27-mediated G1 arrest. Nat Med 8, 1153–1160.

Lim KH, Baines AT, Fiordalisi JJ, Shipitsin M, Feig LA, Cox AD, Der CJ, Counter CM (2005). Activation of RalA is critical for Ras-induced tumorigenesis of human cells. Cancer Cell 7, 533–545.

Lim KH, Brady DC, Kashatus DF, Ancrile BB, Der CJ, Cox AD, Counter CM (2010). Aurora-A phosphorylates, activates and relocalizes the small GTPase RalA. Mol Cell Biol 30, 508–523.

Lim KH, O'Hayer K, Adam SJ, Kendall SD, Campbell PM, Der CJ, Counter CM (2006). Divergent roles for RalA and RalB in malignant growth of human pancreatic carcinoma cells. Curr Biol 16, 2385–2394.

Liu X, Sun Y, Ehrlich M, Lu T, Kloog Y, Weinberg RA, Lodish HF, Henis YI (2000). Disruption of TGF-β growth inhibition by oncogenic Ras is linked to $p27^{Kip1}$ mislocalization. Oncogene 19, 5926–5935.

Livak KJ, Schmittgen TD (2001). Analysis of relative gene expression data using real-time quantitative PCR and the $2^{-\Delta\Delta CT}$ method. Methods 25, 402–408.

Loda M, Cukor B, Tam SW, Lavin P, Fiorentino M, Draetta GF, Jessup JM, Pagano M (1997). Increased proteasome-dependent degradation of the cyclin-dependent kinase inhibitor p27 in aggressive colorectal carcinomas. Nat Med 3, 231–234.

Luo JQ, Liu X, Hammond SM, Colley WC, Feig LA, Frohman MA, Morris AJ, Foster DA (1997). RalA interacts directly with the Arf-responsive, PIP2-dependent phospholipase D1. Biochem Biophys Res Commun 235, 854–859.

Martin TD, Samuel JC, Routh ED, Der CJ, Yeh JJ (2011). Activation and involvement of Ral GTPases in colorectal cancer. Cancer Res 71, 206–215.

Martina JA, Chen Y, Gucek M, Puertollano R (2012). MTORC1 functions as a transcriptional regulator of autophagy by preventing nuclear transport of TFEB. Autophagy 8, 903–914.

Min DS *et al.* (2001). Neoplastic transformation and tumorigenesis associated with overexpression of phospholipase D isozymes in cultured murine fibroblasts. Carcinogenesis 22, 1641–1647.

Montagnoli A, Fiore F, Eytan E, Carrano AC, Draetta GF, Hershko A, Pagano M (1999). Ubiquitination of p27 is regulated by Cdk-dependent phosphorylation and trimeric complex formation. Genes Dev 13, 1181–1189.

Moskalenko S, Henry DO, Rosse C, Mirey G, Camonis JH, White MA (2002). The exocyst is a Ral effector complex. Nat Cell Biol 4, 66–72.

Moskalenko S, Tong C, Rosse C, Mirey G, Formstecher E, Daviet L, Camonis J, White MA (2003). Ral GTPases regulate exocyst assembly through dual subunit interactions. J Biol Chem 278, 51743–51748.

Nakashima S, Nozawa Y (1999). Possible role of phospholipase D in cellular differentiation and apoptosis. Chem Phys Lipids 98, 153–164.

Oft M, Akhurst RJ, Balmain A (2002). Metastasis is driven by sequential elevation of H-ras and Smad2 levels. Nat Cell Biol 4, 487–494.

Oft M, Peli J, Rudaz C, Schwarz H, Beug H, Reichmann E (1996). TGF-β1 and Ha-Ras collaborate in modulating the phenotypic plasticity and invasiveness of epithelial tumor cells. Genes Dev 10, 2462–2477.

Oxford G, Owens CR, Titus BJ, Foreman TL, Herlevsen MC, Smith SC, Theodorescu D (2005). RalA and RalB: antagonistic relatives in cancer cell migration. Cancer Res 65, 7111–7120.

Pagano M, Tam SW, Theodoras AM, Beer Romero P, Del Sal G, Chau V, Renee Yew P, Draetta GF, Rolfe M (1995). Role of the ubiquitin-proteasome pathway in regulating abundance of the cyclin-dependent kinase inhibitor p27. Science 269, 682–685.

Pelish HE, Peterson JR, Salvarezza SB, Rodriguez-Boulan E, Chen JL, Stamnes M, Macia E, Feng Y, Shair MD, Kirchhausen T (2006). Secramine inhibits Cdc42-dependent functions in cells and Cdc42 activation in vitro. Nat Chem Biol 2, 39–46.

Pietenpol JA, Holt JT, Stein RW, Moses HL (1990). Transforming growth factor β1 suppression of c-myc gene transcription: role in inhibition of keratinocyte proliferation. Proc Natl Acad Sci USA 87, 3758–3762.

Reynisdottir I, Massague J (1997). The subcellular locations of $p15^{Ink4b}$ and $p27^{Kip1}$ coordinate their inhibitory interactions with cdk4 and cdk2. Genes Dev 11, 492–503.

Rodier G, Montagnoli A, Di Marcotullio L, Coulombe P, Draetta GF, Pagano M, Meloche S (2001). p27 cytoplasmic localization is regulated by phosphorylation on Ser-10 and is not a prerequisite for its proteolysis. EMBO J 20, 6672–6682.

Rosse C, Hatzoglou A, Parrini MC, White MA, Chavrier P, Camonis J (2006). RalB mobilizes the exocyst to drive cell migration. Mol Cell Biol 26, 727–734.

Sanz-Moreno V, Gadea G, Ahn J, Paterson H, Marra P, Pinner S, Sahai E, Marshall CJ (2008). Rac activation and inactivation control plasticity of tumor cell movement. Cell 135, 510–523.

Schmierer B, Hill CS (2007). TGFβ-SMAD signal transduction: molecular specificity and functional flexibility. Nat Rev Mol Cell Biol 8, 970–982.

Shalom-Feuerstein R, Levy R, Makovski V, Raz A, Kloog Y (2008). Galectin-3 regulates RasGRP4-mediated activation of N-Ras and H-Ras. Biochim Biophys Acta 1783, 985–993.

Shapira KE, Gross A, Ehrlich M, Henis YI (2012). Coated pit-mediated endocytosis of the type I transforming growth factor-β (TGF-β) receptor depends on a di-leucine family signal and is not required for signaling. J Biol Chem 287, 26876–26889.

Sherr CJ, Roberts JM (1999). CDK inhibitors: positive and negative regulators of G1-phase progression. Genes Dev 13, 1501–1512.

Shi Y, Massague J (2003). Mechanisms of TGF-β signaling from cell membrane to the nucleus. Cell 113, 685–700.

Shin I, Yakes FM, Rojo F, Shin NY, Bakin AV, Baselga J, Arteaga CL (2002). PKB/Akt mediates cell-cycle progression by phosphorylation of $p27^{Kip1}$ at threonine 157 and modulation of its cellular localization. Nat Med 8, 1145–1152.

Singhal SS, Singhal J, Yadav S, Dwivedi S, Boor PJ, Awasthi YC, Awasthi S (2007). Regression of lung and colon cancer xenografts by depleting or inhibiting RLIP76 (Ral-binding protein 1). Cancer Res 67, 4382–4389.

Sung TC, Roper RL, Zhang Y, Rudge SA, Temel R, Hammond SM, Morris AJ, Moss B, Engebrecht J, Frohman MA (1997). Mutagenesis of phospholipase D defines a superfamily including a *trans*-Golgi viral protein required for poxvirus pathogenicity. EMBO J 16, 4519–4530.

Tsubari M, Taipale J, Tiihonen E, Keski Oja J, Laiho M (1999). Hepatocyte growth factor releases mink epithelial cells from transforming growth factor β1-induced growth arrest by restoring Cdk6 expression and cyclin E-associated Cdk2 activity. Mol Cell Biol 19, 3654–3663.

Tsukamoto S, Sugio K, Sakada T, Ushijima C, Yamazaki K, Sugimachi K (2001). Reduced expression of cell-cycle regulator $p27^{Kip1}$ correlates with a shortened survival in non-small cell lung cancer. Lung Cancer 34, 83–90.

Ungermannova D, Gao Y, Liu X (2005). Ubiquitination of $p27^{Kip1}$ requires physical interaction with cyclin E and probable phosphate recognition by SKP2. J Biol Chem 280, 30301–30309.

van Dam EM, Robinson PJ (2006). Ral: mediator of membrane trafficking. Int J Biochem Cell Biol 38, 1841–1847.

Viglietto G *et al.* (2002). Cytoplasmic relocalization and inhibition of the cyclin-dependent kinase inhibitor $p27^{Kip1}$ by PKB/Akt-mediated phosphorylation in breast cancer. Nat Med 8, 1136–1144.

Vlach J, Hennecke S, Amati B (1997). Phosphorylation-dependent degradation of the cyclin-dependent kinase inhibitor p27. EMBO J 16, 5334–5344.

Wander SA, Zhao D, Slingerland JM (2011). p27: a barometer of signaling deregulation and potential predictor of response to targeted therapies. Clin Cancer Res 17, 12–18.

Wolfman JC, Palmby T, Der CJ, Wolfman A (2002). Cellular N-Ras promotes cell survival by downregulation of Jun N-terminal protein kinase and p38. Mol Cell Biol 22, 1589–1606.

Wrana JL, Attisano L, Carcamo J, Zentella A, Doodey J, Laiho M, Wang X-F, Massague J (1992). TGFβ signals through a heteromeric protein kinase receptor complex. Cell 71, 1003–1014.

Wu Z, Owens C, Chandra N, Popovic K, Conaway M, Theodorescu D (2010). RalBP1 is necessary for metastasis of human cancer cell lines. Neoplasia 12, 1003–1012.

Xu B, Pelish H, Kirchhausen T, Hammond GB (2006). Large scale synthesis of the Cdc42 inhibitor secramine A and its inhibition of cell spreading. Org Biomol Chem 4, 4149–4157.

Yoon MS, Chen J (2008). PLD regulates myoblast differentiation through the mTOR-IGF2 pathway. J Cell Sci 121, 282–289.

Zeniou-Meyer M *et al.* (2007). Phospholipase D1 production of phosphatidic acid at the plasma membrane promotes exocytosis of large dense-core granules at a late stage. J Biol Chem 282, 21746–21757.